CONTRAST MEDIA & MOLECULAR IMAGING

Received: 31 July 2013, Revised: 16 December 2013, Accepted: 2 February 2014, Published online in Wiley Online Library: 22 April 2014

(wileyonlinelibrary.com) DOI: 10.1002/cmmi.1598

Glycolaldehyde and maleyl conjugated human serum albumin as potential macrophage-targeting carriers for molecular imaging purposes

Björn Gustafsson[a]*, Ulf Hedin[a,b] and Kenneth Caidahl[a,c]

Maleylated bovine serum albumin is a known ligand for targeting macrophages and has potential as a carrier for molecular imaging purposes. We present a novel synthesis of glycolaldehyde-conjugated human serum albumin (GA-HSA) and maleylated human serum albumin (Mal-HSA). Seventeen modifications of fluorescently tagged GA-HSA and Mal-HSA molecules with different degrees of conjugation were prepared. The comparative uptake studies, using 12 of these modifications, were done *in vitro* on mouse monocytes/macrophages (RAW264.7), and evaluated qualitatively by confocal microscopy and quantitatively by flow cytometry. The GA modifications are taken up by the macrophages approximately 40% better than the maleyl modifications at low concentrations (≤3 μM), while at higher concentrations it appears that the maleyl modifications are taken up around 25–44% better than the GA-modified HSA. However, high uptake at low concentrations will be beneficial for *in vivo* localizing inflammation in areas with low penetration of the probe as in an atherosclerotic plaque. Further, another advantage of GA-HSA is that GA competes less than the maleyl group for the free reactive amine sites that are to be used for conjugation of metal chelating ligands (e.g. tetraazacyclododecanetetraacetic acid and triazacyclononanetriacetic acid). Metal ions such as Gd^{3+} and Mn^{2+} can be chelated for positive Magnetic Resonance (MR) contrast and positron emitting ions such as $^{64}Cu^{2+}$ and $^{68}Ga^{3+}$ for Positron Emission Tomography (PET) imaging. These are important properties, especially, when considering the MR contrast possibilities owing to the low sensitivity of the technique, and would motivate the use of GA-HSA before Mal-HSA. © 2014 The Authors. *Contrast Media & Molecular Imaging* published by John Wiley & Sons, Ltd.

Keywords: molecular imaging; cellular targeting; fluorescent probes; atherosclerosis; contrast agent; glycolaldehyde; human serum albumin; MRI; PET

1. INTRODUCTION

With the growing interest in molecular imaging of inflammation in general, and atherosclerotic inflammation in particular, shown by many recent publications (1–12), there is a need for new imaging probes of the various modalities now available for atherosclerosis imaging. Novel probes will need to be more specifically targeted to the cells, enzymes or antigens of interest in order to appear promising in the clinical field. Atherosclerosis is established as a progressive, chronic, inflammatory disease (13,14) with major fatal danger lying in the formation of labile and vulnerable plaques prone to rupture (15–17), causing thrombosis. Currently, the gold standard of clinical atherosclerosis imaging is based on visualization of vessel stenosis and plaque morphology, so the important biological information at the cellular level is somewhat limited and needs to be addressed. It has been shown that the danger of plaque depends neither on the sheer size nor the degree of stenosis, but rather on the cellular composition of the plaque (15–17). A highly vulnerable plaque has a thin fibrous cap and elevated levels of inflammatory cells such as monocyte-derived macrophages, T-lymphocytes, mast cells and lipid-laden foam cells where at least the macrophages and lymphocytes are already present from the early stages of the disease (18). Macrophages are identified as one of the most important cellular components in formation and destabilization of plaques and are, therefore, interesting as targets for new imaging probes (19). Several scavenger receptors are over-expressed on the plaque macrophage surfaces and have a broad ligand specificity for a large variety of polyanionic macromolecules, for example, maleylated bovine serum albumin (Mal-BSA) (20,21) and glycolaldehyde conjugated bovine serum albumin (GA-BSA) (21–25). Mal-BSA, and other

* *Correspondence to: B. Gustafsson, Center for Molecular Medicine, Department of Molecular Medicine and Surgery, Karolinska Institutet, Stockholm, Sweden. E-mail: bjorn.gustafsson@ki.se*

a *B. Gustafsson, U. Hedin, K. Caidahl*
Center for Molecular Medicine, Department of Molecular Medicine and Surgery, Karolinska Institutet, Stockholm, Sweden

b *U. Hedin*
Department of Vascular Surgery, Karolinska University Hospital, Stockholm, Sweden

c *K. Caidahl*
Department of Clinical Physiology, Karolinska University Hospital, Stockholm, Sweden

modified albumins, have also been shown to target scavenger receptors on macrophages in different types of malignant tumours (26–28) as well as scavenger receptors on sinusoidal liver endothelial cells (29). Modified albumins used as carriers of signal providing moieties have previously also been shown useful for imaging of macrophages by Gustafsson *et al.* (30) and by Tawakol *et al.* (31). With a well-designed imaging probe there is a potential to target macrophages in atherosclerotic plaques, or other inflamed tissues, using these modified albumins and thereby detect early signs of disease. Therefore, we studied the uptake in macrophages of glycolaldehyde-conjugated human serum albumin (GA-HSA) and maleylated human serum albumin (Mal-HSA) by means of flow cytometry and confocal microscopy.

2. MATERIALS AND METHODS

2.1. General

All chemicals and reagents were purchased from Sigma-Aldrich (St. Louis, MO, USA) unless otherwise stated. HSA (≥96%), GA dimer, racemate (crystalline), maleic anhydride (Mal-A) (Fluka, ≥99.0%), fluorescein isothiocyanate (FITC) (FluoroTag™-kit), Pacific Blue™ succinimidyl ester (PB; (Invitrogen, Molecular Probes, Eugene, OR, USA), 2-[N-(7-nitrobenz-2-oxa-1,3-diazol-4-yl) amino]-2-deoxy-D-glucose (2-NBDG; Invitrogen, Molecular Probes), 4′,6-diamidine-2′-phenylindole, dihydrochloride (DAPI; >99%, KPL, Gaithersburg, MD, USA), tetramethylammonium hydroxide (25% sol.), phosphoric acid (≥85%), dimethyl sulfoxide (DMSO), anhydrous (≥99.5%) and 1X phosphate buffered saline (PBS) (pH 7.4, Gibco, Paisley, UK) were used as purchased without further purification.

In order to determine the optimal reaction conditions for the syntheses of GA-HSA and Mal-HSA, a range of different molar ratios between the modifying ligand and HSA were used. Molar ratios used for GA:HSA were between 151:1 and 1409:1 and for Mal-A:HSA, they ranged between 174:1 and 621:1.

We synthesized and used for confocal microscopy studies the following probes: GA_9-HSA-FITC$_n$, GA_{16}-HSA-FITC$_n$, Mal_{41}-HSA-FITC$_n$, Mal_{54}-HSA-FITC$_n$ and HSA-FITC$_n$ with varying and unknown degrees of FITC conjugations. For flow cytometry the following probes were synthesized: GA_{40}-HSA-$FITC_{1.8}$, GA_{74}-HSA-$FITC_{1.8}$, GA_{23}-HSA-PB_{29}, Mal_{28}-HSA-$FITC_{1.8}$, Mal_{38}-HSA-$FITC_{1.8}$, Mal_{46}-HSA-$FITC_{2.4}$ and HSA-$FITC_{1.8}$. GA_{16}-HSA-FITC$_n$, Mal_{38}-HSA-FITC$_n$, Mal_{41}-HSA-FITC$_n$, Mal_{54}-HSA-FITC$_n$ and Mal_{56}-HSA-FITC$_n$ were also prepared and used in pilot experiments. The subscript number after GA, Mal, FITC or PB indicates the number of GA, Mal, FITC or PB moieties in each conjugate; the subscript *n* varies from 0.5 to 5. Numbers of GA, Mal, FITC and PB groups, respectively, indicate an average number of conjugated groups per HSA.

2.2. Preparation and fluorescence labelling of GA-HSA

The methods used by Nagai *et al.* (24) were followed and GA was conjugated to mainly the free, accessible lysyl amines but also to the arginyl amines, by formation of a Schiff base (24). A typical preparation proceeded as follows: 50 mg (~0.75 μmol) HSA was dissolved in 25 ml 1× PBS and solid glycolaldehyde dimer was added in portions during stirring at ambient temperature. The pH was monitored and it changed from ~7.9 to ~8.0 by the addition of GA dimer. Stirring was continued for approximately 48 h and the final pH was 7.7. The solution was filtered using a 0.2 μm filter and then purified on a custom made 13 mm × 185 mm Sephadex G-50 desalting column with distilled demineralized water (ddH_2O) as eluent. The product was then lyophilized before further analysis. The fluorescence labelling with FITC followed the protocol in the labelling kit and was verified by UV–vis spectrophotometry (Shimadzu UV mini 1240, Shimadzu, Kyoto, Japan). The amount of fluorophore bound to each HSA molecule was determined by matrix-assisted laser desorption ionization mass spectrometry (MALDI-MS). For the flow cytometry studies the GA-conjugation was made using a batch of FITC pre-labeled HSA in order to ensure equal amounts of fluorescent groups on all modifications. For the flow cytometry analysis of the competition study, HSA was first labeled with PB, following a typical procedure. Then 10 mg (~0.15 μmol) HSA was dissolved in 2.0 ml 0.1 M sodium bicarbonate buffer, pH 8.65, and 200 μl solution of ~2 mg PB in anhydrous DMSO was added drop-wise while continuously stirring at ambient temperature for 3.5 h. The solution was then purified on a custom-made 13 mm × 185 mm Sephadex G-50 desalting column with ddH_2O as eluent and the product lyophilized before further analysis. The HSA-PB was then conjugated with GA, following the procedure described above (molar ratio GA:HSA; 663:1). The number of bound fluorophores was determined by MALDI-MS.

2.3. Preparation and fluorescence labelling of Mal-HSA

By following a modification of a method described by Butler and Hartley (32), maleyl groups were conjugated, at different degrees, to the free and accessible lysyl and arginyl amines on the protein, through the formation of an amide bond. A typical preparation proceeded as follows: 50 mg (~0.75 μmol) HSA was dissolved in 25 ml 0.1 M tetramethylammonium phosphate buffer, pH 9.00 at ambient temperature, and solid Mal-A was added in portions. The solution was stirred and pH was kept within the range of 8.5–9.0 by drop-wise additions of 2.5% tetramethylammonium hydroxide solution. After approximately 10 min, the reaction was complete, indicated by no further release of acid and a constant pH of 8.6. Immediately after the reaction, the solution was purified on a custom-made 13 mm × 185 mm Sephadex G-50 desalting column with ddH_2O as eluent. Thereafter, samples were lyophilized before further analysis. The fluorescence labelling followed the protocol in the FITC-labelling kit and was verified by UV–vis spectrophotometry. For the flow cytometry studies, the maleyl conjugations were made using FITC pre-labeled HSA in order to ensure equal amounts of fluorescent groups on all modifications. Bound amount of FITC was determined by MALDI-MS.

2.4. Mass spectrometry

MS (Applied Biosystems Voyager DE-PRO MALDI-TOF, Foster City, CA, USA) was used to analyze the number of GA, Mal, FITC and PB groups that were conjugated to the HSA and to determine the molecular mass of the final products. A sample preparation of 0.5 μl of the analyte (10 pmol/μl in 0.1% formic acid, was mixed with 0.5 μl saturated sinapinic acid solution in a 1:2 mixture of acetonitrile –0.1% trifluoroacetic acid. The droplet on the target plate was dried at room temperature before analysis on a target plate and the sample was analyzed by MALDI and the resulting ions analyzed by time-of-flight mass spectrometry. By comparisons between the average molecular mass of the different HSA-modifications with that of the pure HSA, an approximate average number of GA, Mal, FITC and PB groups could be determined. The method accuracy was estimated to ±300 g/mol.

2.5. Cell studies

2.5.1. Confocal microscopy

RAW264.7 mouse monocytes/macrophages were seeded on gelatine coated eight-chambered well-slides at a density of ~100 000 cells/well and incubated for 24 h in 400 μl serum-free RPMI-1640 medium supplemented with insulin, transferrin and selenium medium (ITS-medium). Four different fluorescent HSA-based agents – GA_9-HSA-$FITC_n$, GA_{16}-HSA-$FITC_n$, Mal_{41}-HSA-$FITC_n$ and Mal_{54}-HSA-$FITC_n$, a non-modified negative control – with HSA-$FITC_n$ and 2-NBDG dissolved in 400 μl ITS medium were applied, at different concentrations, to the cells, which were incubated for 15 min at 37 °C. Cells were then washed with 3 × 500 μl 1× PBS, fixated with zinc formaldehyde for 15 min and incubated for another 10 min with DAPI for nuclei staining. The slides were then mounted for confocal microscopy where the uptake of the fluorescent probe was studied. Images were obtained on a Leica TCS SP5 system (Leica Microsystems, Wetzlar, Germany) using 488 nm as the excitation wavelength.

2.5.2. Flow cytometry

As a first experiment, B1, to quantify the cellular uptake of the probe, the cells were seeded on 12-well plates at a density of ~500 000 cells/well and incubated for ~6 h in 2 ml serum-free RPMI-1640 medium supplemented with ITS-medium and then incubated with 1 ml of four different probe solutions – GA_{40}-HSA-$FITC_{1.8}$, GA_{74}-HSA-$FITC_{1.8}$, Mal_{28}-HSA-$FITC_{1.8}$ and Mal_{38}-HSA-$FITC_{1.8}$ – at five different concentrations in ITS-medium for 15 min at 37 °C. The cells were then washed with 3 × 2 ml 1× PBS and scraped off, collected and separated from the medium and re-suspended in 1 ml 1× PBS and analyzed by flow cytometry using a Dako Cytomation CyAn™ ADP Analyzer flow cytometer (Dako, Glostrup, Denmark) with an excitation wavelength of 488 nm. Uptake was evaluated for agents conjugated with GA and with Mal groups using the concentrations from 0 to 11.9 μM. Nonconjugated HSA-$FITC_{1.8}$ was used as negative control. Comparisons were also done using the fluorescent glucose analog 2-NBDG, to resemble the uptake of ^{18}F-fluorodeoxyglucose commonly used for PET-imaging.

A second experiment, B2, a competition study between two probe modifications – GA_{23}-HSA-PB_{29} and Mal_{46}-HSA-$FITC_{2.4}$ – was then undertaken. The cells were seeded on 12-well plates at a density of ~500 000 cells/well and incubated for ~6 h in 2 ml serum-free RPMI-1640 medium supplemented with ITS-medium, and then simultaneously incubated with the two probes in one solution of 1.5 ml ITS-medium for 15 min at 37 °C at six different concentrations, 0–15 μM. The cells were then washed with 3 × 2 ml 1× PBS and scraped off, collected and separated from the medium and re-suspended in 1 ml 1× PBS, then analyzed by flow cytometry using the same system as above, with excitation wavelengths of 488 nm for the FITC-conjugated Mal-HSA and 405 nm for the PB-conjugated GA-HSA.

3. RESULTS

3.1. Probes

Our probes are based on HSA acting as a carrier of the imaging active moiety. For recognition by macrophages, HSA can be modified by groups making the conjugate polyanionic such as with maleyl groups by conjugation with Mal-A or by GA conjugation.

The resulting purified probes were analyzed by MS (MALDI-TOF, *m/z*): A (M^+, 100) HSA, 66 654; GA_9-HSA, 67 220; GA_{16}-HSA, 67 593; Mal_{41}-HSA, 70 627; Mal_{54}-HSA, 71 996. The FITC-labelling of these probes was verified by UV–vis. B1 (M^+, 100) HSA, 66 580; HSA-$FITC_{1.8}$, 67 288; GA_{40}-HSA-$FITC_{1.8}$, 69 691; GA_{74}-HSA-$FITC_{1.8}$, 71 741; Mal_{28}-HSA-$FITC_{1.8}$, 70 032; Mal_{38}-HSA-$FITC_{1.8}$, 71 040. B2 (M^+, 100) HSA, 66 570; HSA-PB_{29}, 73 084; HSA-$FITC_{2.4}$, 67 484; GA_{23}-HSA-PB_{29}, 74 489; Mal_{46}-HSA-$FITC_{2.4}$, 71 252.

The outcomes of the conjugation reactions were found somewhat difficult to unambiguously interpret, and the degree of conjugation was difficult to predict and control accurately with only molar ratios. MS analyses of all the different probes demonstrated variable degrees of conjugation but correlations between ligand:HSA molar ratios and number of conjugated ligands were observed.

3.2. Cell studies

In order to evaluate the cellular uptake of the probes, the mouse monocyte/macrophage cell line RAW264.7 was employed. Uptake was examined by confocal microscopy and flow cytometry.

3.2.1. Confocal microscopy

For nice clear visualization of the molecular uptake *in vitro*, several different probes were prepared for confocal microscopy imaging. The images presented in Fig. 1 are examples of the uptake of two different GA-modifications and two different maleyl modifications. Cells were incubated with different concentrations of the compounds and uptake of the agent could be verified as well as differences in the uptake depending on the type of modification and concentration by just looking at the images.

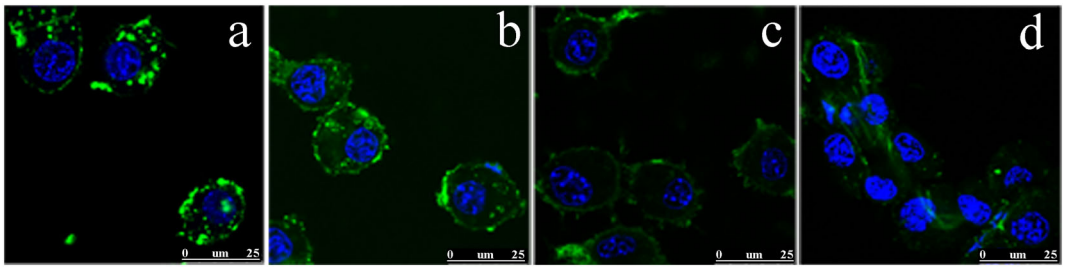

Figure 1. Confocal microscopy images of RAW264.7 cells at 189× magnification showing (a) 10 μM GA_9-HSA-FITC, (b) 50 μM GA_{16}-HSA-FITC, (c) 50 μM Mal_{41}-HSA-FITC and (d) 50 μM Mal_{54}-HSA-FITC incubated for 15 min at 37 °C. The green colour represents the FITC-labelled compound and the blue colour represents the 4′,6-diamidine-2′-phenylindole, dihydrochloride (DAPI) nucleus stain.

3.2.2. *Flow cytometry*

In B1, four different fluorescently FITC-labelled probes (1.8 FITC per HSA determined by MALDI-MS) were synthesized and modified with varying degrees of GA and maleyl groups to facilitate the analyses. The flow cytometry analyses showed a concentration-dependent uptake of all HSA-modifications and virtually no uptake of the deoxyglucose analog control 2-NBDG. They also showed a 4- to 6-fold increase in uptake of both types of modification compared with the nonmodified FITC-labelled HSA as seen in Fig. 2. Up to a probe concentration of approximately 5 μM the uptake of the GA-conjugated HSA compounds was shown to be ~20–100% higher than that of the Mal-HSA conjugates. At higher probe concentrations the Mal_{38}-HSA uptake deviated from the linear behavior and uptake increased significantly, while the GA_{74}-HSA uptake decreased at similar concentration.

In B2, two different probes were synthesized (FITC- or PB-labelled) and both probes showed simultaneous uptake, with approximately 40% higher uptake for GA-HSA than for Mal-HSA below the concentration of 3 μM. However, above that concentration, the Mal-HSA outcompeted the other modification and, at ~15 μM, Mal-HSA was taken up at a ~44% higher degree of total uptake than GA-HSA as shown in Fig. 3.

4. DISCUSSION

BSA molecules modified with, for example, maleyl- or malondialdehyde groups are known to target macrophages through their surface scavenger receptors, especially the class A scavenger receptors (SR-A) (21). Additionally, Nagai *et al*. indicates that modifications of BSA with GA are also recognized by SR-A as active ligands (24). The purpose of this study was to compare the GA modification with the maleyl modification, aiming to evaluate its efficiency in order to be taken up by macrophages *in vitro*. Thus, the GA-modification could possibly prove to be a better choice as a targeted carrier of PET- and/or MR-active metals than the previously reported imaging probe Mal_x-BSA-[2-(4-isothiocyanatobenzyl)-1,4,7,10-tetraazacyclododecane-1,4,7,10-tetraacetic

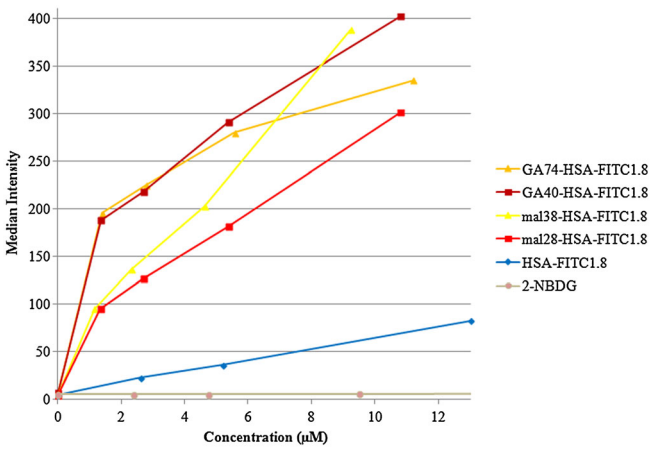

Figure 2. Diagram, obtained from the flow cytometry analysis, showing the cellular uptake as median fluorescence intensity of HSA-fluorescein isothiocyanate (FITC), maleylated human serum albumin (Mal-HSA)-FITC, glycolaldehyde conjugated human serum albumin (GA-HSA)-FITC and 2-[*N*-(7-nitrobenz-2-oxa-1,3-diazol-4-yl) amino]-2-deoxy-D-glucose as a function of concentration. Incubations on RAW264.7-cells were performed for 15 min at 37 °C.

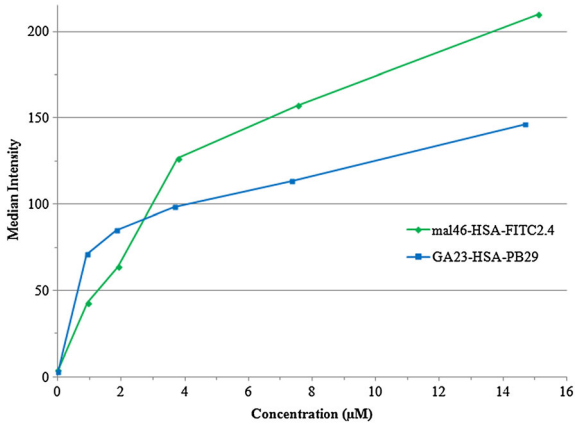

Figure 3. Diagram, obtained from the flow cytometry analysis, showing the simultaneous, competitive cellular uptake as median fluorescence intensity of Mal-HSA-FITC and GA-HSA-Pacific Blue™ succinimidyl ester as a function of concentration. Incubations on RAW264.7 cells were performed for 15 min at 37 °C.

acid-$(Gd)]_y$ {Mal_x-BSA-[*p*-SCN-Bz-DOTA-$(Gd)]_y$} (30). Assuming that HSA and BSA are interchangeable for this purpose, we used HSA instead of BSA to create a probe that is more adapted for future human use.

The fluorophores as well as the prospective metal chelators, in these cases *S*-2-(4-isothiocyanatobenzyl)-1,4,7-triazacyclononane-1,4,7-triacetic acid (*p*-SCN-Bz-NOTA) or *p*-SCN-Bz-DOTA, for the PET- and/or MR-active metals, also react with the lysyl amine groups and thus compete for the same sites as the maleyl and the GA groups. For MRI purposes, owing to the low sensitivity of the technique, it is important to have many paramagnetic centers per molecule. Therefore, the number of free amine sites available for conjugation with the metal chelator is of greatest importance. This is not as important for PET imaging since the technique is extremely sensitive and it only demands a much lower number of bound positron emitters to provide enough signal. The GA binds to both lysyl and arginyl amine groups and by following the synthesis by Nagai *et al*. (24) the GA leaves ~12–16 free lysyl residues. The Mal-A BSA-modification reaction (32) is shown to only leave ~3 free lysyl amine groups (33); therefore GA competes less strongly with FITC, PB or the metal chelators than Mal-A does, leaving more available lysyl amine sites. This would be a benefit to the imaging properties of the probe, especially for MR-imaging.

4.1. Probes

Plain HSA has 60 amine sites that originate from the lysine amino acids, and 27 amine sites originating from the arginine amino acids, which are theoretically available (34). The maleyl groups as well as the GA groups bind to both the lysyl and arginyl amines but maleyl occupies ~20% more of the free lysyl amine sites (33) than the GA (24), possibly owing to less steric hindrance. The moieties necessary for imaging properties that is, FITC, PB, *p*-SCN-Bz-NOTA or *p*-SCN-Bz-DOTA will also be bound to the lysyl amines utilizing the isothiocyanate group that can form a thiourea bond, or for PB using the succinimidyl ester group to form an amide bond, with the primary amines. For the fluorescence imaging, that moiety is the FITC or the PB and we plan to use *p*-SCN-Bz-NOTA or *p*-SCN-Bz-DOTA for chelation of a suitable positron-emitting metal.

Previously it has been shown that, the higher the degree of maleylation, the higher the cellular uptake and that a ~60% maleylation degree (~36 maleyl groups per molecule of BSA) of BSA is optimal to balance with a sufficient amount of gadolinium in order to present useful relaxivity values for MRI (30). A modification that utilizes other amine sites or less of the lysyl amine sites for conjugation would enable more free sites for conjugation of the imaging contrast providing groups, which would make it easier to conjugate groups necessary for binding gadolinium ions for the less sensitive MR-imaging and give higher cellular uptake at lower concentrations. This theory was initially the reason for investigating the albumin derivatization with glycolaldehyde and comparison with the well-studied maleyl conjugation of albumin (20,21).

4.2. Cell studies

4.2.1. Confocal microscopy

The likely differences in the number of conjugated FITC molecules (0.5–5 FITC/HSA) between the probes synthesized initially make it difficult to conclude which probe is actually taken up the most. Visual examination indicated that the GA-modifications were taken up to a greater degree than the maleyl modifications (Fig. 1). However, since a highly conjugated (with GA or Mal) HSA has fewer sites that are free for FITC conjugation than a lower conjugated one, it is possible that this can result in lower fluorescence intensities. The concentration dependence of the uptake of the different probes is thus difficult to determine, and a matter of subjectivity, to quantitatively evaluate by visual inspection of microscopy images; therefore, analysis using flow cytometry was employed.

4.2.2. Flow cytometry

This technique counts and measures the size and granularity of cells and correlates that to their fluorescence. The uptake concentration dependency for each probe can then be evaluated by plotting the median fluorescence intensity against the different probe concentrations.

The dependence on the amount of maleyl groups seems to be concomitant with results from a previous publication (30), that is, the more maleyl groups the higher the cellular uptake. For the GA modification, this difference seems very small, at least below 6 μM. By comparison of the two types of modification, it could be observed that, for the lower concentrations (<5 μM), GA modified HSA is taken up at a higher degree, 20–100%, than Mal-HSA. At higher concentrations, conclusions from the uptake are more uncertain since the higher modified HSAs seem to deviate slightly from the apparent trends of the lower modified agents. Considering the Mal_{38}-HSA-$FITC_{1.8}$, it is clear that uptake increases in a concentration-dependent manner and that uptake is higher than that of the less conjugated Mal_{28}-HSA-$FITC_{1.8}$, as shown (30). For GA_{74}-HSA-$FITC_{1.8}$, the decrease of uptake at concentrations above 5 μM might occur because cells get saturated with the agent earlier owing to the larger spatial size. A limitation of the study might be that the distribution of differently conjugated HSA molecules in the same batch makes it difficult to know exactly which molecular modification is actually taken up in the highest amount. Most likely, they are all taken up but with slightly different affinities toward the cellular receptors.

Compared with the modified HSA conjugates, the uptake of HSA-$FITC_{1.8}$ was very low, which was expected, and the uptake of 2-NBDG was negligible. Possibly the cells needed to be immune activated or more metabolically active in order to show uptake of a glucose analog like this fluorescent deoxyglucose.

To evaluate which modification has the strongest affinity to the SR-A of the cells, a competition study was performed where both the Mal-HSA and GA-HSA were added to the cells. This experiment showed a higher average uptake of the GA-conjugated HSA at lower (≤3 μM) concentrations but an increasing uptake of maleyl conjugated HSA at higher concentrations. A higher uptake at lower concentration levels could be beneficial when it comes to targeting and visualizing areas of low-grade inflammation or with reduced circulation and probe access as in atherosclerotic plaques. In such a case the GA-modified HSA would be preferred. A possible explanation for the lower macrophage uptake of GA-HSA than Mal-HSA at high probe concentrations might be the lower degree of conjugation of GA to the HSA; furthermore, the relatively high amounts of the PB fluorophore possibly could affect the uptake values negatively owing to its size. There might be a possibility that conjugation of the tentative metal chelating moieties, that is, *p*-SCN-Bz-NOTA or *p*-SCN-Bz-DOTA, to HSA could also affect the cellular uptake in a negative way owing to their size and amounts of up to 30 molecules per HSA. However, previous uptake studies in macrophages of Mal_{36}-BSA $(Gd\text{-}DOTA)_n$ ($10 \leq n \leq 22$) have shown that uptake of the modified BSA occurs even with 22 Gd-coordinated DOTA-moieties (30).

5. CONCLUSION

The GA-modifications appear to be taken up better by the RAW264.7-cells than the maleyl modifications at lower probe concentrations. This would be a definite advantage in situations with low expected probe concentrations *in vivo*, applying molecular imaging for instance to detect inflammation in atherosclerotic plaques. Another advantage of GA-HSA would be that GA seems to compete less than maleyl for the free reactive amine sites of HSA which will be used for binding contrast providing moieties. These important features, especially considering the future use of MR contrast, where enhanced binding of sufficient amounts of contrast and optimal uptake in regions of interest are very important, will help overcome the low sensitivity of the technique. Keeping the injected dosage to a minimum is, of course, also preferable. These theoretical advantages, in conjunction with the results of our uptake studies, might motivate *in vivo* exploration of the potential benefit of GA-HSA over Mal-HSA.

Acknowledgements

Financial support was provided by the Swedish Heart Lung Foundation, the Swedish Research Council, Karolinska Institutet, Tore Nilson's Foundation for Medical Research and the Stockholm County Council.

REFERENCES

1. Briley-Saebo KC, Shaw PX, Mulder WJM, Choi SH, Vucic E, Aguinaldo JG, Witztum JL, Fuster V, Tsimikas S, Fayad ZA. Targeted molecular probes for imaging atherosclerotic lesions with magnetic resonance using antibodies that recognize oxidation-specific epitopes. Circulation 2008; 117: 3206–3215.

2. Choudhury RP, Fisher EA. Molecular imaging in atherosclerosis, thrombosis, and vascular inflammation. Arterioscler Thromb Vasc Biol 2009; 29: 983–991.
3. Cormode DP, Skajaa T, Fayad ZA, Mulder WJM. Nanotechnology in medical imaging: probe design and applications. Arterioscler Thromb Vasc Biol 2009; 29: 992–1000.
4. Fayad ZA. Cardiovascular molecular imaging. Arterioscler Thromb Vasc Biol 2009; 29: 981–982.
5. Jaffer FA, Libby P, Weissleder R. Optical and multimodality molecular iImaging insights into atherosclerosis. Arterioscler Thromb Vasc Biol 2009; 29: 1017–1024.
6. Kraitchman DL, Bulte JWM. In vivo imaging of stem cells and beta cells using direct cell labeling and reporter gene methods. Arterioscler Thromb Vasc Biol 2009; 29: 1025–1030.
7. Langer H, Schonberger T, Bigalke B, Gawaz M. Where is the trace? Molecular imaging of vulnerable atherosclerotic plaques. Semin Thromb Hemost 2007; 33: 151–158.
8. Laufer EM, Winkens MHM, Narula J, Hofstra L. Molecular imaging of macrophage cell death for the assessment of plaque vulnerability. Arterioscler Thromb Vasc Biol 2009; 29: 1031–1038.
9. Nahrendorf M, Weissleder R. Advances in cardiovascular medicine through molecular imaging. Radiology 2007; 47: 18–24.
10. Rudd JHF, Hyafil F, Fayad ZA. Inflammation imaging in atherosclerosis. Arterioscler Thromb Vasc Biol 2009; 29: 1009–1016.
11. Tang TY, Muller KH, Graves MJ, Li ZY, Walsh SR, Young V, Sadat U, Howarth SP, Gillard JH. Iron oxide particles for atheroma imaging. Arterioscler Thromb Vasc Biol 2009; 29: 1001–1008.
12. Villanueva FS. Molecular imaging of cardiovascular disease using ultrasound. J Nucl Cardiol 2008; 15: 576–586.
13. Libby P. Inflammation in atherosclerosis. Nature 2002; 420: 868–874.
14. Ross R. Mechanisms of disease – atherosclerosis – an inflammatory disease. New Engl J Med 1999; 340: 115–126.
15. Carr S, Farb A, Pearce WH, Virmani R, Yao JST. Atherosclerotic plaque rupture in symptomatic carotid artery stenosis. J Vasc Surg 1996; 5: 755–66.
16. Virmani R, Burke AP, Kolodgie FD, Farb A. Pathology of the thin-cap fibroatheroma. J Interv Cardiol 2003; 16: 267–272.
17. Virmani R, Burke AP, Kolodgie FD, Farb A. Vulnerable plaque: the pathology of unstable coronary lesions. J Interv Cardiol 2002; 15: 439–446.
18. Hansson GK. Inflammation, atherosclerosis, and coronary artery disease. New Engl J Med 2005; 352: 1685–1695.
19. Moreno PR, Falk E, Palacios IF, Newell JB, Fuster V, Fallon JT. Macrophage infiltration in acute coronary syndromes – implications for plaque rupture. Circulation 1994; 90: 775–778.
20. Ottnad E, Via DP, Frubis J, Sinn H, Friedrich E, Ziegler R, Dresel HA. Differentiation of binding-sites on reconstituted hepatic scavenger receptors using oxidized low-density-lipoprotein. Biochem J 1992; 281: 745–751.
21. Platt N, Gordon S. Is the class A macrophage scavenger receptor (SR-A) multifunctional? – The mouse's tale. J Clin Invest 2001; 108: 649–654.
22. Higai K, Satake M, Nishioka H, Azuma Y, Matsumoto K. Glycated human serum albumin enhances macrophage inflammatory protein-1[beta] mRNA expression through protein kinase C–[delta] and NADPH oxidase in macrophage-like differentiated U937 cells. Biochim Biophys Acta Gen Subj 2008; 1780: 307–314.
23. Horiuchi S, Sakamoto Y, Sakai M (eds). Scavenger Receptors for Oxidized and Glycated Proteins. Springer: Vienna, 2001.
24. Nagai R, Matsumoto K, Ling X, Suzuki H, Araki T, Horiuchi S. Glycolaldehyde, a reactive intermediate for advanced glycation end products, plays an important role in the generation of an active ligand for the macrophage scavenger receptor. Diabetes 2000; 49: 1714–1723.
25. Nagai R, Mera K, Nakajou K, Fujiwara Y, Iwao Y, Imai H, Murata T, Otagiri M. The ligand activity of AGE-proteins to scavenger receptors is dependent on their rate of modification by AGEs. Biochim Biophys Acta Mol Basis Dis 2007; 1772: 1192–1198.
26. Anatelli F, Mroz P, Liu Q, Yang C, Castano AP, Swietlik E, Hamblin MR. Macrophage-targeted photosensitizer conjugate delivered by intratumoral injection. Mol Pharm 2006; 3: 654–664.
27. Liu Q, Hamblin MR. Macrophage-targeted photodynamic therapy: scavenger receptor expression and activation state. Int J Immunopathol Pharmacol 2005; 18: 391–402.
28. Hamblin MR, Miller JL, Ortel B. Scavenger-receptor targeted photodynamic therapy. Photochem Photobiol 2000; 72: 533–540.
29. Duryee MJ, Freeman TL, Willis MS, Yang C, Hunter CD, Hamilton BC III, Suzuki H, Tuma DJ, Klassen LW, Thiele GM. Scavenger receptors on sinusoidal liver endothelial cells are involved in the uptake of aldehyde-modified proteins. Mol Pharmacol 2005; 68: 1423–1430.
30. Gustafsson B, Youens S, Louie AY. Development of contrast agents targeted to macrophage scavenger receptors for MRI of vascular inflammation. Bioconjug Chem 2006; 17: 538–547.
31. Tawakol A, Castano AP, Gad F, Zahra T, Bashian G, Migrino RQ, Ahmadi A, Stern J, Anatelli F, Chirico S, Shirazi A, Syed S, Fischman AJ, Muller JE, Hamblin MR. Intravascular detection of inflamed atherosclerotic plaques using a fluorescent photosensitizer targeted to the scavenger receptor. Photochem Photobiol Sci 2008; 7: 33–39.
32. Butler PJG, Hartley BS. Maleylation of Amino Groups. Methods in Enzymology. Academic Press: London, 1972; 191–199.
33. Alaiz M, Beppu M, Ohishi K, Kikugawa K. Modification of delipidated apoprotein-B of low-density-lipoprotein by lipid oxidation-products in relation to macrophage scavenger receptor-binding. Biol Pharm Bull 1994; 17: 51–57.
34. UniProt, UniProtKB. Available from: http://www.uniprot.org/uniprot/P02768 [14 November 2013].